JOURNAL OF OPTOELECTRONICS AND ADVANCED MATERIALS, Vol. 11, No. 8, August 2009, p. 1111 - 1116

Sapphire, SiC, AlN, Si and diamond-substrate material for GaN HEMT and LED

BHUBESH CHANDER JOSHI*, C. DHANAVANTRI, D. KUMAR[a]

Optoelectronic Devices Group, Central Electronics Engineering Research Institute (Council of Scientific and Industrial Research),Pilani (Rajasthan), 333031 India

[a]*Electronic Science Department, Kurukshetra University, Kurukshetra*

Performance of AlGaN/GaN High Electron Mobility Transistor on Sapphire, Si, AlN, SiC and Diamond substrates are studied. AlGaN/GaN HEMT on Sapphire shows negative differential conductivity region, at large drain bias, due to large accumulation of heat in channel at gate drains edge. Remarkable improvement in characteristics is observed for HEMT devices on high thermal conducting SiC and Diamond substrate. No significant improvements in characteristics are observed for HEMT structure on Si and AlN substrate. Effect of rise in junction temperature of GaN LED on Sapphire is analyzed. Results show that, there is accumulation of heat in area between two electrodes.

(Received 09, July 2009; accepted August 05, 2009)

Keywords: HEMT, LED, GaN, InGaN, AlGaN

1. Introduction

III-N material based devices have gained more attention, due to their good thermal conductivity, high breakdown field (GaN ~3 x 10^6 V/cm) and high saturation velocities (GaN ~3 x 10^7 cm/s) [1]. These devices can operate at high temperature, without degradation in performance. Reliability, performance and life time combination of these devices are much higher than any other material based devices. The Polarization field in III-V materials are larger than others III-V compound semiconductor. GaN based devices are showing great performance in field of power and optoelectronic. The performance level of AlGaN/GaN HEMTs devices are increasing rapidly from last few years. Output power densities of 30W/mm [2] for AlGaN/GaN HEMT device on SiC were achieved and AlGaN/GaN amplifier with 1kW at 3.2GHz was reported [3]. At present, GaN based LEDs are used for a variety of applications, including back lighting of liquid crystal displays, traffic signals, full color displays, and white LEDs. High efficiency white LEDs have potential to replace fluorescent lamps.

GaN based devices are facing many problems due to non-availability of bulk GaN material. So there structures are hetero-epitaxially grown on foreign substrate. GaN devices are general grown on SiC [4, 5], Si [6, 7, 8] and Sapphire [9, 10, 11, 12] by MOCVD or MBE. SiC is most suitable material for these devices, with lattice mismatch of 3 %. But the main drawback of SiC is its high cost. Composite SiC substrate are showing promise candidate for GaN devices. SiC on poly crystal SiC shows same level of performance as of single crystal SiC substrate [13, 14], and can be a promising candidate for GaN HEMT. Recently researchers have been attracted to diamond substrate [15] due to its large thermal conductivity (10 to 30 W/(cm-K)). Dislocation density in GaN buffer grown on Sapphire are order of 10^{9-10} cm^{-2}[16, 17], and GaN buffer grow on SiC shows 10^8dislocations per cm^2 [18]. These dislocation centers acts as non radiative centers and degrades the output performance of LED. Introduction of low temperature nucleation layer [19], annealing [20], Fe [21], delta doping [22, 23] greatly improved the quality of GaN epitaxial layer. High quality epitaxial layer with low dislocation density and semi insulating buffer, are primary need, for GaN based power and optoelectronic devices.

Self heating at large bias is commonly observed in high power devices. Generated heat must be conducted out from the active region to maintain performance of device. Thus thermal conductivity of the substrates plays a significant role in the device performance and reliability. In this work, different substrate materials for AlGaN/GaN HEMT are studied at high drain bias, by ATLAS, a commercially available software package from Silvaco. It is very important to determine the junction temperature of the LED during operation. Performance of AlGaN/InGaN/GaN LED structure on Sapphire and SiC are studied by ATLAS.

2. Simulation approach

HEMT and LED structure used in this study are shown in Fig. 1 and Fig. 2 respectively. Parameters used in simulation are listed in Table 1. For AlGaN/GaN HEMT gate length is 0.7 μm. Gate to source and gate to drain spacing are 1 and 1.1 μm respectively. Aluminum composition (x) in AlGaN/GaN HEMT is 0.30. For LED

Aluminum and Indium composition in AlGaN and InGaN are 0.20.

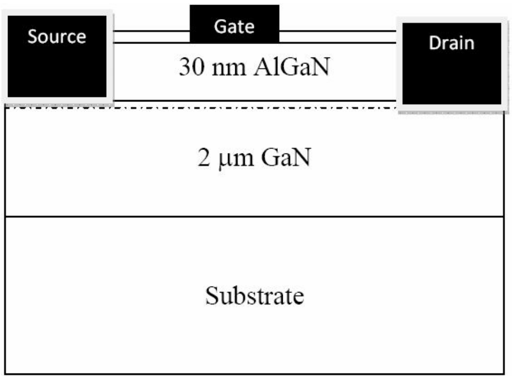

Fig.1 Structure of AlGaN/GaN HEMT.

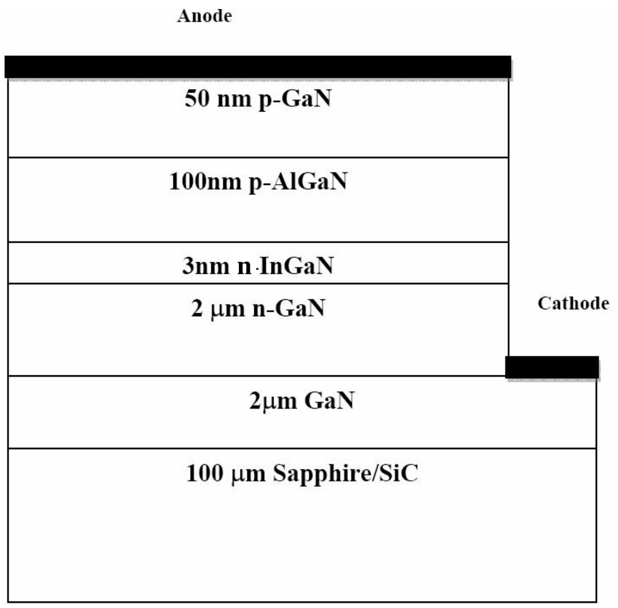

Fig. 2. Structure of AlGaN/InGaN/GaN LED.

Temperature dependent thermal conductivity model is used for AlGaN/GaN HEMT and LED and its form is

$$k(T) = (a + bT + cT^2)^{-1} \quad (1)$$

where a, b and c are thermal constants.

Band gap of III-N semiconductors at temperature T is given by.

$$Eg(T) = Eg(0) - m^*T^2/(T+n) \quad (2)$$

where Eg (T) is Bandgap of semiconductor at temperature T, Eg(0) is bandgap at 0K and m, n are thermal constants.

For ternary compounds

$$Eg_{(AxB(1-x)N)} = Eg_{(AN)}x + Eg_{(BN)}(1-x) - q^*x(1-x \quad (3)$$

where x is mole fraction of ternary semiconductor and q is bowing parameter.

For GaN m = 0.909 x 10^{-3}, n = 830

And for AlGaN bowing parameter (q) is 1.3

Spontaneous and piezoelectric induced charges are the major source of carriers in GaN based hetero-junction devices [24]. Polarization charges at interface are given by

$$Pint = Ptotal(Top\ layer) - Ptotal(bottom\ layer) \quad (5)$$

and

$$Ptotal = Spontaneous\ polarization + Piezoelectric\ Polarization \quad (6)$$

Spontaneous polarization of GaN is -0.034 C/m^2 and for AlGaN layer is given by [25]

$$P_{sp} = -0.09x - 0.034(1-x) + 0.021x_n(1-x) \quad (7)$$

And piezoelectric polarization in strained AlGaN grown on GaN is given by

$$P_{pz} = -0.0525x + 0.0282 \times (1-x) \quad (8)$$

Thin $Al_{0.3}GaN_{0.7}N$ epitaxial layer grown on GaN experience biaxial tensile stress and net polarization charge at interface is given by

$$Pint(AlGaN/GaN) = 1.38 \times 10^{-13}\ cm^{-2}$$

3. Results and discussion

I-V characteristics curve of AlGaN/GaN HEMT on Sapphire are shown in Fig. 3. Maximum channel current of 857mA/mm is obtained for HEMT on Sapphire. Maximum transconductance of 201mS/mm is obtained for HEMT on Sapphire.

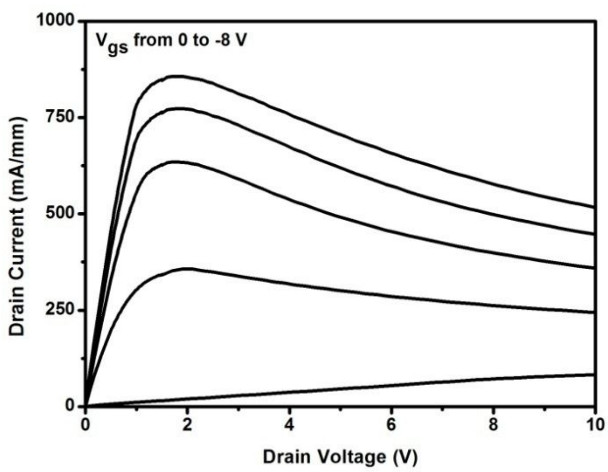

Fig. 3. I-V Curves of AlGaN/GaN on sapphire.

Thermal analysis of AlGaN/GaN HEMT on sapphire shows large accumulation of heat in channel near gate edge of drain side Fig. 4. Channel temperature rises to 683K for V_{ds} > 15V. The large accumulation of heat in channel is due to poor thermal conductivity of Sapphire. For HEMT on SiC, a remarkable improvement in device characteristics is obtained. Maximum channel current of 993mA/mm is obtained for AlGaN/GaN HEMT on SiC.

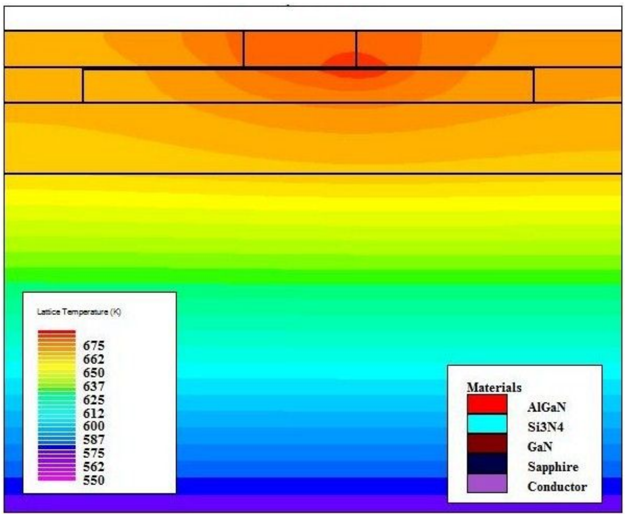

Fig. 4. AlGaN/GaN HEMT on sapphire.

Further improvement in channel current is observed for AlGaN/GaN HEMT on Diamond Fig. 5. Maximum channel current of 1566mA/mm is obtained for HEMT on Diamond.

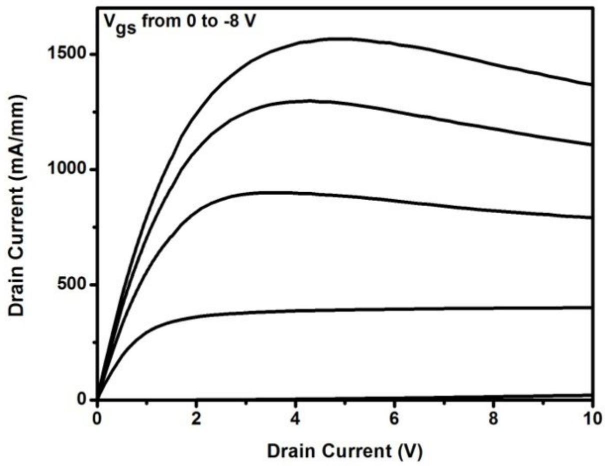

Fig. 5. I-V Curves of AlGaN/GaN on diamond.

AlGaN/GaN HEMT on AlN and Si does not show any improvement Fig. 6. Maximum transconductance of 273mS/mm and 213 mS/mm is obtained for HEMT on Diamond and SiC respectively. In pinch off condition, drain current falls to zero for HEMT on Diamond, but for HEMT on Sapphire channel current does not fall to zero even after Vgs = -10V Fig. 7. This result shows that thermal noise is generated in HEMT, due to device heating. Transfer curve for AlGaN/GaN on different substrates are shown Fig. 8.

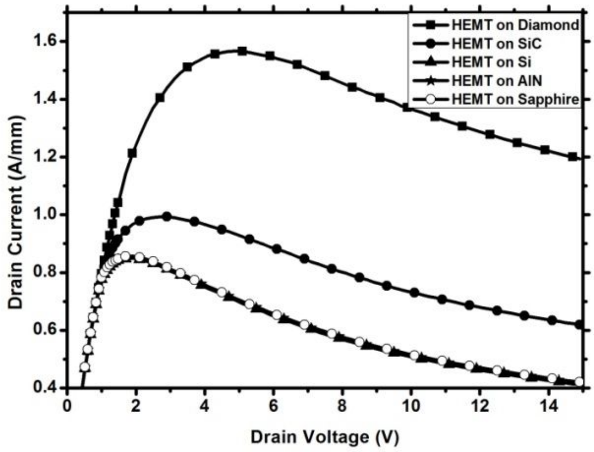

Fig. 6. I-V Curves of AlGaN/GaN HEMT on different substrates at V_{gs}=0V.

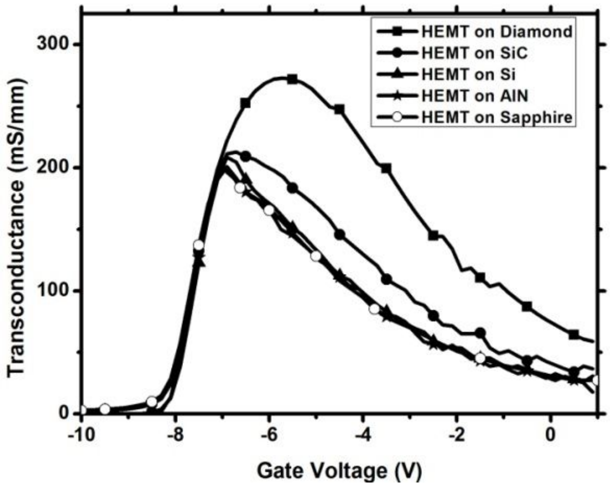

Fig. 7. Transconductance for AlGaN/GaN HEMT on different substrates.

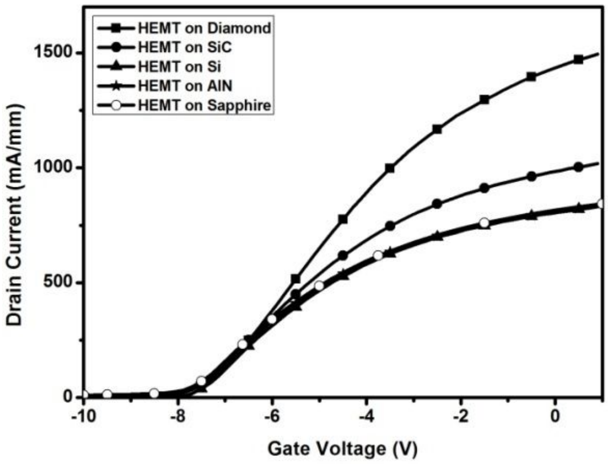

Fig. 8. Transfer curve for AlGaN/GaN HEMT on different substrates.

AlGaN/InGaN/GaN LED structure on Sapphire and SiC substrate (Fig. 2) are studied by ATLAS. Device parameters used in this study are given in Table 1. These improvements in device characteristics on SiC and Diamond can directly correlate with channel temperature as shown in Fig. 9.

Table 1. HEMT and LED materials parameter used in this study.

Parameters	Value
Interface charge	$1.38x10^{13}$ /cm^2
Thermal contact	300 K
Thermal conductivity of diamond	20 W/(cm-K)
ΔEc/ΔEv (Band Offset)	0.7/0.3
Thermal resistance at substrate	200 W/(cm^2-K)
GaN Electron mobility	300 cm^2/(V-s)
Schottky barrier height of gate metal	1.23 eV
Electron saturation velocity(AlGaN)	$1.12\ x10^7$ cm/s
Electron saturation velocity (GaN)	$1.91\ x10^7$ cm/s
Band Gap $Al_{.3}Ga_{.7}N$	3.97 eV
LED area	350 * 350 μm^2

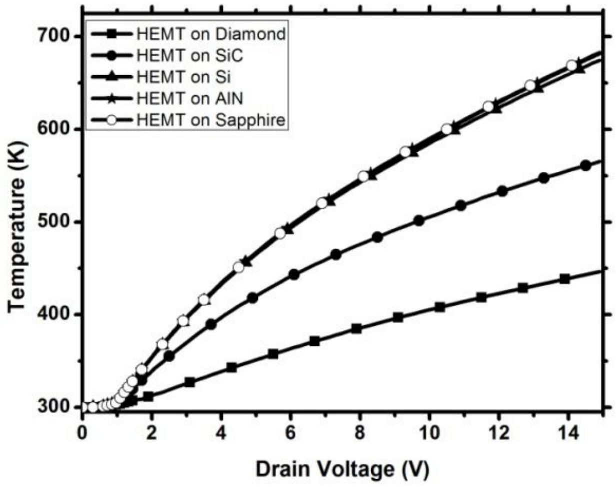

Fig. 9. Transfer curve for AlGaN/GaN HEMT on different substrates.

Fig. 10 shows the channel temperature of AlGaN/GaN HEMT on Diamond falls to 446K.

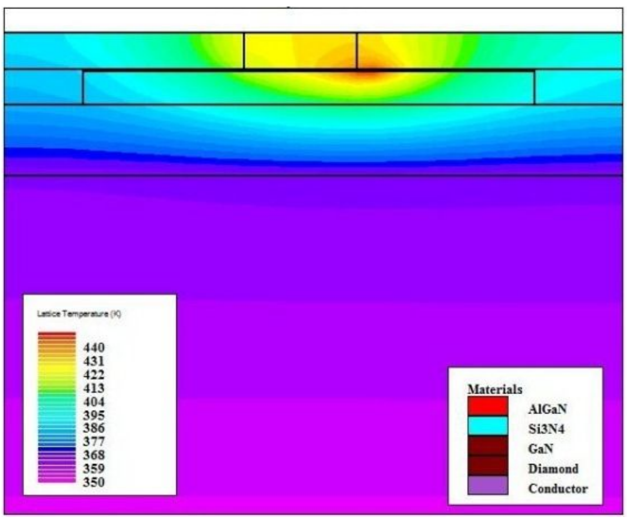

Fig. 10. AlGaN/GaN HEMT on diamond.

Results extracted from AlGaN/GaN HEMT on different substrates are shown in Table 2.

Table 2. Results extracted from AlGaN/GaN HEMT devices on different substrates.

Substrate	Max. channel current (mA/mm)	Channel temperature (K) at V_{ds}=15V and V_{gs}=0V	Channel temperature (K) at V_{ds}=3V and V_{gs}=1V	Maximum transconductance (mS/mm)	Threshold voltage (V)
Diamond	1566	446	325	273	-8
SiC	993	565	370	213	-8
Si	850	674	395	208	-8
AlN	855	682	397	201	-8
Sapphire	857	683	396	201	-8

Thermal analysis results shows that maximum heating is observed, in the area between two electrodes, and the temperature rises to 330K for LED structure on Sapphire biased at 10V Fig. 11.

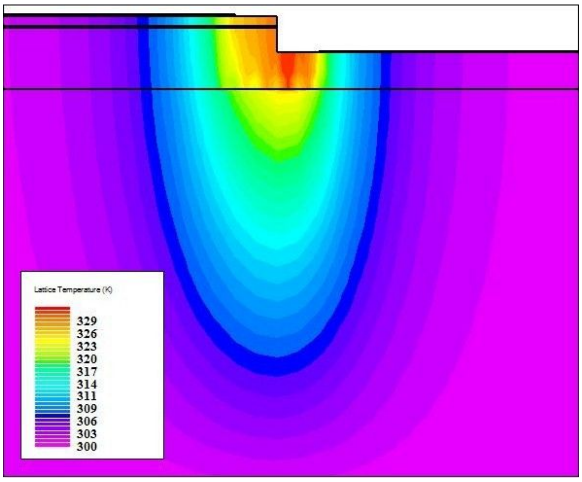

Fig. 11. AlGaN/InGaN/GaN LED on sapphire (V_{anode} = 10 V).

By changing the substrate from Sapphire to SiC the maximum temperature in this region falls to 320K. I-V curves of LED structure on Sapphire and SiC substrate are shown in Fig. 12. Very little improvement in anode current is observed for device on SiC. Electroluminescence (EL) curve of LED structure on Sapphire and SiC are shown in Fig. 13. No change in EL peak is observed.

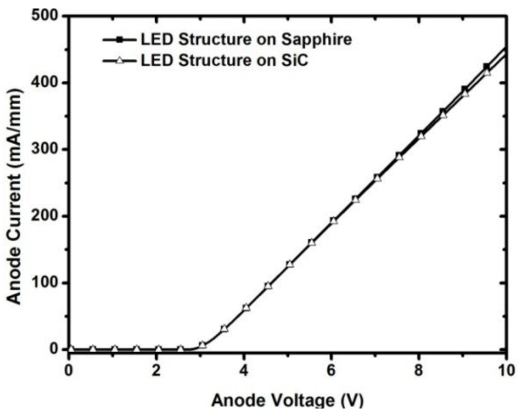

Fig. 12. I-V Curves for AlGaN/InGaN/GaN LED on sapphire and SiC.

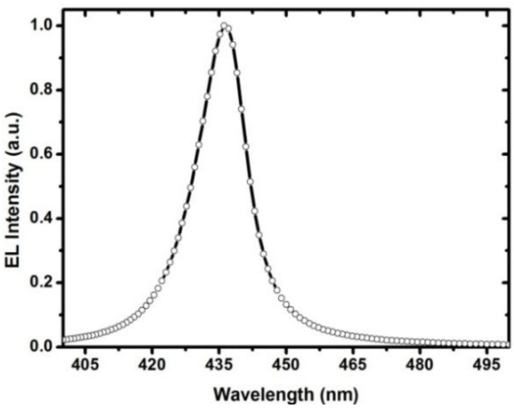

Fig. 13. EL Curve for AlGaN/InGaN/GaN LED on sapphire/SiC.

Variation of temperature of device with anode current is shown in Fig. 14.

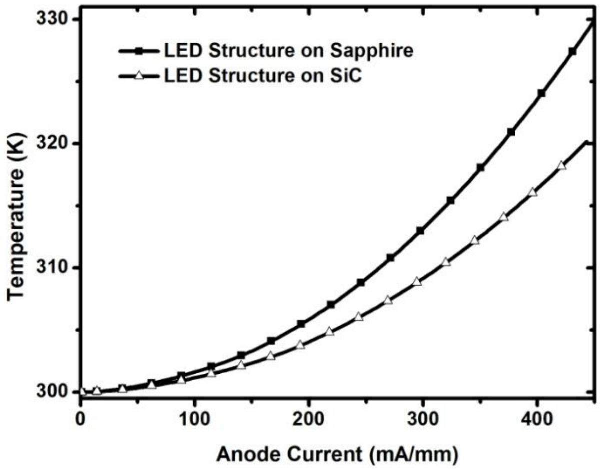

Fig. 14. Variation of LED device temperature with respect to anode voltage.

4. Conclusions

Effects of high thermal conducting substrate materials on performance of AlGaN/GaN HEMT and AlGaN/InGaN/GaN LED devices are studied by ATLAS. AlGaN/GaN HEMT on sapphire shows maximum drain current of 857mA/mm. I-V curves of AlGaN/GaN HEMT on sapphire shows large negative differential region at higher drain bias. Thermal analysis of the device shows, a large accumulation of heat in channel at gate edge. Great improvement in channel current is observed for device on high thermal conductive substrate. Maximum channel current of 0.993A/mm and 1.57A/mm is observed for HEMT on SiC and Diamond respectively. Maximum transconductance of 201mS/mm, 213mS/mm and 273mS/mm are observed for HEMT on Sapphire, SiC and Diamond respectively. No improvement in output characteristics are observed for device on Si and AlN substrate. Thermal analysis of AlGaN/InGaN/GaN LED on Sapphire shows that, large accumulation of heat in area between two electrodes. Very little improvement in performance is obtained for AlGaN/InGaN/GaN LED on SiC substrate. In conclusion the heat generated inside the device, have very impact on device performance and this heat must be extracted out to maintain the performance of device. High thermal conductive substrate material have great impact in AlGaN/GaN HEMT and must be employed in device manufacturing to achieve maximum performance from the device.

Acknowledgements

One of the authors, Bhubesh Chander Joshi acknowledges the Council of Scientific and Industrial Research (CSIR), New Delhi, for the award of SRF

(NET), and also acknowledges all member of Optoelectronics Devices Group for their support.

References

[1] U. K. Mishra, Y.-F. Wu, B. P. Keller, S. Keller, S. P. Denbaars, IEEE Trans Microwave Theory Techniques **46**, 756 (1998).

[2] Y.-F. Wu, A. Saxler, M. Moore, R. P. Smith, S. Sheppard, P. M. Chavarkar, T. Wisleder, U. K. Mishra, P. Parikh, Electron Device Letter **25**, 117 (2004).

[3] E. Mitani, M. Aojima, S. Sano, IEEE-Microwave integrated circuit conference, 2007, eumic 2007, european, October 176, 2007.

[4] S. Rajan, P. Waltereit, C. Poblenz, S. J. Heikman, D. S. Green, J. S. Speck, U. K. Mishra, IEEE Electron Device Letter **25**, 247 (2004).

[5] J. W. Johnson, J. Han, A. G. Baca, R. D. Briggs, R. J. Shul, J. R. Wendt, C. Monier, F. Ren, B. Luo, S. N. G. Chu, D. Tsvetkov, V. Dmitriev, S. J. Pearton, Solid State Electronics **46**, 513 (2002).

[6] S. Pal, C. Jacob, Bulletien of material science **27**, 501 (2004).

[7] S. Iwakami, O. Machida, M. Yanagihara, T. Ehara, N. Kaneko, H. Goto, A. Iwabuchi, Japanese J. of applied Physics, **46**, L587 (2007).

[8] C.-T. Liang, Kuang Yao Chen, N. C. Chen, P. H. Chang, Chin-An Chang, Applied Physics Letter **89**, 132107 (2006).

[9] D. S. Wuu, W. K. Wang, K. S. Wen, S. C. Huang, S. H. Lin, S. Y. Huang, C. F. Lin, R. H. Horng, Applied Physics Letters **89**, 161105 (2006).

[10] X. Q. Shen, H. Okumura, K. Furuta, N. Nakamura, Applied Physics Letters **89**, 171906 (2006).

[11] S. Raghavan, J. M. Redwing, J. of Applied Physics **96**, 2995 (2004).

[12] V. Soukhoveev, O. Kovalenkov, L. Shapovalova, V. Ivantsov, A. Usikov, V. Dmitrie, V. Davydov, A. Smirnov, Phys. Stat. Sol. (c) **3**, 1483 (2006).

[13] G. Meneghessol, C. Ongarol, E. Zanonil, C. Brylinski, M. A. di Forte-Poisson, V. Hoet, J. C. de Jaeger, R. Langer, H. Lahreche, P. Bove4, J. Thorpe IEDM, **1**, 401 (2007).

[14] V. Hoel, N. Defrance, J. C. De Jaeger, H. Gerard, C. Gaquiere, H. Lahreche, R. Langer, A. Wilk, M. Lijadi, S. Delage, Electronics Letters **44**, 238 (2008).

[15] J. G. Felbinger, M. V. S. Chandra, Y. Sun, Lester F. Eastman, J. Wasserbauer, F. Faili, D. Babic, D. Francis, F. Ejeckam, IEEE Electron Device Letters **28**, 948 (2007).

[16] H.-M. Wang, J.-P. Zhang, C.-Q. Chen, Q. Fareed, J.-W. Yang, M. Asif Khan, Applied Physics Letter **81**, 604 (2002).

[17] J. Chaudhuri, J. T. George, J. of material Science **37**, 1449 (2002).

[18] K. Murakawa, E. Niikura, F. Hasegawa, H. Kawanishi, Japanese J. of Applied Physics **46**, 3301 (2007).

[19] Akasaki, H Amano, Y. Koide, K. Hiramatsu, N. Sawaki, J. of Crystal Growth **98**, 209 (1989).

[20] C. F. Lin, G. C. Chi, M. S. Feng, J. D. Guo, J. T. Tsang, J. M. Hong, Applied Physics Letter **68**, 3758 (1996).

[21] C. C. Young, C. H.-Young, G. S. Michael, F. Eastman Lester, IEEE Transactions on Electron Devices **53**, 2926 (2006).

[22] Y. B. Pan, Z. J. Yang, Z. T. Chen, Y. Lu, T. J. Yu, X. D. Hu, K.. Xu, G. Y. Zhang, J. of Crystal Growth **286**, 255 (2006).

[23] H. Lahre Che, P. Venne Gue, B. Beaumont, P. Gibart, J. of Crystal Growth **205**, 245 (1999).

[24] J. P. Ibbeton, P. T. Fini, K. D. Ness, S. P. DenBaars , J. S. Speck, U. K. Mishra, Applied Physics Letter **77**, 250 (2000).

[25] C. Wood, D. Jena, O. Ambacher , V. Cimalla, Polarization Effects in Semiconductors **2**, 44, Springer Press New York, 2008.

*Corresponding author: bhubesh25@gmail.com